

# Synthesis, structure and impedance spectroscopic analysis of $[(\text{Pb}_x\text{Sr}_{1-x})\cdot\text{OTiO}_2]_{64}[(2\text{SiO}_2\cdot\text{B}_2\text{O}_3)]_{25}[\text{BaO}]_7[\text{K}_2\text{O}]_3[\text{La}_2\text{O}_3]_1$ glass ceramic system doped with $\text{La}_2\text{O}_3$

C. R. Gautam · Prabhakar Singh · O. P. Thakur ·  
D. Kumar · O. Parkash

Received: 26 March 2012 / Accepted: 21 May 2012 / Published online: 6 June 2012  
© Springer Science+Business Media, LLC 2012

**Abstract** Various compositions of glasses were prepared by melt quenching method in the glass ceramic  $64[(\text{Pb}_x\text{Sr}_{1-x})\text{OTiO}_2]_{64}[(2\text{SiO}_2\cdot\text{B}_2\text{O}_3)]_{25}[\text{BaO}]_7[\text{K}_2\text{O}]_3[\text{La}_2\text{O}_3]_1$  ( $0.5 \leq x \leq 1$ ) system doped with  $\text{La}_2\text{O}_3$ . Dielectric constant,  $\epsilon_r$  versus temperature,  $T$ , plots revealed diffused peaks, while dielectric loss,  $D$ , versus  $T$  plots showed shifting in the peaks toward the higher temperature side similar to relaxor-like ceramics. Curie temperature was found to change systematically with changing the concentration of SrO. Impedance spectroscopy results indicated the contributions of polarization process relaxing in low frequency region attributed to polarizations at the crystal to glass interface and the glassy region.

## Introduction

Ferroelectric glass ceramics are technologically important materials. The properties and applications of glass ceramics depend on the complex inter-relationship of structural,

compositional, and processing variables [1]. Ferroelectric ceramics have been applied to many electronic and optical devices by utilizing their excellent dielectric, piezoelectric, and optical properties [2]. Recently considerable attention has been focused on the development of the technology for their crystal growth and high dielectric constant in bulky glass ceramic samples. These glass ceramics possess interesting dielectric properties resulting from the combination of high permittivity crystallites and low permittivity glassy matrix. Impedance spectroscopy technique [3, 4] can be better exploited to understand the mechanism responsible for interesting dielectric and crystallization behavior.  $\text{SrTiO}_3$  (ST) borosilicate glass ceramic system has been investigated extensively for their crystallization microstructural and dielectric behavior [5–8]. Crystallization study of this glass ceramic system shows that  $\text{Sr}_2\text{B}_2\text{O}_5$  forms a major crystalline phase followed by  $\text{Sr}_3\text{Ti}_2\text{O}_7$ ,  $\text{TiO}_2$ , and some other phases. Different additives to the glass composition affect crystallization, microstructural, and dielectric behavior of resulting glass ceramics. Sahu et al. [9, 10] reported that  $(\text{PbSr})\text{TiO}_3$  (PST) solid solution crystallites can be crystallized in borosilicate glassy matrix. The crystal structure and lattice parameters of these crystallites of perovskite phase change systematically with changing  $\text{Pb}^{2+}/\text{Sr}^{2+}$  ratio in the glass compositions. The dielectric behavior of these glass ceramic samples shows that Curie temperature,  $T_c$  increases with increasing  $\text{Pb}^{2+}/\text{Sr}^{2+}$  ratio [11, 12]. But these glass ceramics find limited applications because of their low dielectric constant ( $\epsilon_r$ ) (of the order of 100). It has been reported that  $\text{La}_2\text{O}_3$  promotes the crystallization of perovskite phase [13].  $\text{La}_2\text{O}_3$ -doped ST glass ceramics show high value of  $\epsilon_r$  of the order of 1,000 due to space charge polarization at crystal–glass interface. Recently, Kumar et al. [14] have reported dielectric characterization of ferroelectric  $(\text{Pb}_x\text{Sr}_{1-x})\text{TiO}_3$

---

C. R. Gautam (✉)  
Department of Physics, University of Lucknow, Lucknow  
226007, India  
e-mail: gautam\_ceramic@yahoo.com

P. Singh  
Department of Applied Physics, Institute of Technology,  
Banaras Hindu University, Varanasi 221005, India

O. P. Thakur  
Solid State Physics Laboratory, Lucknow Road, Timarpur,  
Delhi 110054, India

D. Kumar · O. Parkash  
Department of Ceramic Engineering, Institute of Technology,  
Banaras Hindu University, Varanasi 221005, India

glass ceramics doped with  $\text{La}_2\text{O}_3$ , showing improved crystallization and dielectric characteristics.

The electrical properties of glass ceramics are due to a result of different contributions from various components and processes present in the materials. In general, the overall dielectric properties arise due to crystallites, glassy interface and electrode processes. The motion of charge could take place in any fashion viz. charge displacement, dipole reorientation and space charge formation [15]. In order to achieve reproducibility and to have a proper control over these properties, contributions from the crystalline phase, glassy matrix, and contact electrode must be separated out. The method of complex immittance analysis has emerged as a very powerful tool for separating out these contributions [3]. It is also useful in studying defects, microstructure, surface chemistry and electrical conductivity for materials including dielectrics, ionic conductors, and adsorbate–adsorbent interfaces [16]. Under an AC field, frequency dispersion or dielectric relaxation is observed due to different polarization mechanisms [17]. The presence of a dielectric relaxation then corresponds to a possible polarization mechanism, which occurs on a macroscopic scale. Each relaxation process may be characterized by a relaxation time, which describes the decay of a particular polarization process with time on removing the external field. Experimentally more than one relaxation process can be observed in the frequency range of interest. Certain dielectric functions are employed more often than others depending on the particular field of application. For example, electric modulus is generally used for glasses [18] while impedance is chosen for polycrystalline ionic conductors. Various studies on the crystallization behavior and dielectric properties of glass ceramics containing crystalline phase such as  $\text{PbTiO}_3$  have been reported [19–28]. Recently research work has been carried out on  $(\text{Sr}_{1-x}\text{Pb}_x)\text{TiO}_3$  glass ceramics with addition of  $\text{Nb}_2\text{O}_5$  for dielectric and impedance spectroscopic studies [29]. More recently in a letter by our group, we have reported dielectric characterization of ferroelectric glass ceramic system  $[(\text{Pb}_x\text{Sr}_{1-x})\text{O}\cdot\text{TiO}_2]-[2\text{SiO}_2\cdot\text{B}_2\text{O}_3]-[\text{K}_2\text{O}]-[\text{BaO}]-[\text{La}_2\text{O}_3]$  ( $0.5 \leq x \leq 1$ ), showing improved crystallization and dielectric characteristics [30]. Doping of  $\text{La}_2\text{O}_3$  influenced dielectric constant value causing a considerable enhancement in its value. In view of the fact that the addition of 1 %  $\text{La}_2\text{O}_3$  enhances the crystallization of the glasses and therefore, acting as a nucleating agent, it was planned to synthesize a few compositions of  $64[(\text{Pb}_x\text{Sr}_{1-x})\text{O}\cdot\text{TiO}_2]-25[(2\text{SiO}_2\cdot\text{B}_2\text{O}_3)]-7[\text{BaO}]-3[\text{K}_2\text{O}]$  glass ceramic system doped with  $\text{La}_2\text{O}_3$  and study their dielectric and impedance behavior with respect to temperature and frequency scales. In this paper, we present our detailed investigation on electrical and dielectric properties of the system  $64[(\text{Pb}_x\text{Sr}_{1-x})\text{O}\cdot\text{TiO}_2]-25[(2\text{SiO}_2\cdot\text{B}_2\text{O}_3)]-7[\text{BaO}]-3[\text{K}_2\text{O}]$

doped with  $\text{La}_2\text{O}_3$  for relatively high concentration of substituent, i.e.,  $0.5 \leq x \leq 1$ . A few glass ceramic samples in of this system have been selected for the dielectric study. The prime goal of this work is to determine the characteristics of impedance and crystallization behavior of PST borosilicate glass ceramic system.

## Experimental procedure

A series of glasses in the system  $64[(\text{Pb}_x\text{Sr}_{1-x})\text{O}\cdot\text{TiO}_2]-25[2\text{SiO}_2\cdot\text{B}_2\text{O}_3]-7[\text{BaO}]-3[\text{K}_2\text{O}]-1[\text{La}_2\text{O}_3]$  were prepared by progressive substitution of SrO for PbO ( $x = 1.0, 0.9, 0.8, 0.7, 0.6$ , and  $0.5$ ). Well mixed, dried powders containing appropriate amounts of reagent grade PbO,  $\text{SrCO}_3$ ,  $\text{TiO}_2$ ,  $\text{H}_3\text{BO}_3$ ,  $\text{SiO}_2$ ,  $\text{K}_2\text{CO}_3$ , and  $\text{La}_2\text{O}_3$  were melted in pure alumina crucibles for an hour in the temperature range  $1,210$ – $1,240$  °C, depending on the composition, under normal atmospheric conditions. The melt was quenched by pouring it onto an aluminum mold and pressing with a thick aluminum plate. The glasses were then annealed at  $400$  °C for 3 h. Differential thermal analysis (DTA) was done using a NETZSCH Simultaneous Thermal Analyzer (STA-409) from room temperature ( $\sim 27$  °C) to  $1,400$  °C employing a heating rate of  $10$  °C/min to determine glass transition,  $T_g$  and crystallization temperatures,  $T_c$ . Sintered alumina was used as a reference material. On the basis of DTA results, various glass ceramic samples with compositions  $x = 1.0$ – $0.5$  were prepared by heat treatment of the glasses in the temperature range  $605$ – $1,060$  °C for 6 h. The different heat treatment schedules and nomenclature of glass ceramic samples are listed in the Table 1. Five letters glass code refers to the composition of the glass. First two letters PT, 9P, etc., designate the fraction of lead, i.e.,  $x$  in the glass system. PT refers to  $x = 1.0$ , i.e., 100 % lead (Pb) and 0 % strontium. 9P, 8P, etc., refer to  $x = 0.9, 0.8$ , etc., respectively. The third letter L indicates that  $\text{La}_2\text{O}_3$  is used as an additive. The last two letters 7B refers to fraction of modifier oxides BaO in the parent glass compositions. For the nomenclature of the glass ceramic samples following methodology has been adopted: First five letters in the code for the glass ceramic samples are similar to the code of their parent glass and refer to the composition of glass, next three digits indicate the crystallization temperature. The last letter T or S refers to holding time at crystallization temperature, 3 and 6 h, respectively. For example, the glass ceramic code PTL7B663T represents the glass ceramic sample which has been prepared from the glass PTL7B containing 100 % lead, 1 %  $\text{La}_2\text{O}_3$  and BaO/ $\text{K}_2\text{O}$  ratio of 7/3 and heat treated at  $663$  °C for 3 h. Phases were identified using powder X-ray diffraction (XRD) analysis. Diffraction patterns were recorded employing a Rigaku

**Table 1** Heat treatment schedule, glass and glass ceramic codes and crystalline phases of different glass ceramic samples in the system  $64[(\text{Pb}_x\text{Sr}_{1-x})\text{O}\cdot\text{TiO}_2]-25[2\text{SiO}_2\cdot\text{B}_2\text{O}_3]-7[\text{BaO}]-3[\text{K}_2\text{O}]-1[\text{La}_2\text{O}_3]$

	Glass code	Glass ceramic code	Heat treatment schedules			Crystalline phases
			Heating rate (°C/min)	Holding time (h)	Holding temp (°C)	
<i>P</i> Perovskite titanate, <i>PT</i> $\text{PbTi}_3\text{O}_7$ , <i>R</i> rutile ( $\text{TiO}_2$ )	PTL7B	PTL7B663T	5	3	663	P + PT + R
		PTL7B663S	5	6	663	P + PT
	9PL7B	9PL7B680T	5	3	680	P + PT
		9PL7B680S	5	6	680	P + PT
	8PL7B	8PL7B775T	5	3	775	P + PT
		8PL7B775S	5	6	775	P + PT
	7PL7B	7PL7B790T	5	3	790	P + PT
		7PL7B790S	5	6	790	P + PT
	6PL7B	6PL7B796T	5	3	796	P+PT
		6PL7B796S	5	6	796	P+PT
	5PL5B	5PL7B781S	5	3	781	P + PT
		5PL7B781S	5	6	781	P + PT + R

X-ray diffractometer using  $\text{CuK}_\alpha$  radiation. The crystalline phases in each glass ceramic sample were identified by comparing its XRD pattern with standard patterns of various crystalline phases. The glass ceramic samples were ground and polished successively using SiC powders on a thick and flat glass plate. Finally polishing was carried out on a blazer cloth using diamond paste (1  $\mu\text{m}$ ). The polished glass ceramic samples were etched for 1 min with a suitable etchant 30 %  $\text{HNO}_3$  + 20 % HF solution. Etched surface of various glass ceramic samples were coated with Gold by sputtering method. The samples were then examined using a JSM-840 scanning electron microscope (SEM) to study the morphology of different crystalline phases. Capacitance (*C*) and dissipation factor (*D*) were recorded as a function of temperature between room temperature and 500 °C at 0.1, 1, 10 kHz and 1 MHz using an HP 4284A precision LCR meter. The impedance measurements were carried out as a function of frequency (0.01 Hz–3 MHz) using a Novo Control  $\alpha$ -S High Resolution Dielectric Analyzer. The values of capacitance *C*, dielectric loss *D*, conductance *G*, real and imaginary impedance  $Z'$  and  $Z''$  were measured as a function of frequency at various temperatures. Complex impedance and modulus plots ( $Z''$  vs.  $Z'$  and  $M''$  vs.  $M'$ ) were drawn for a few compositions. Based on the complex plane impedance and modulus plots, equivalent electrical circuit, models representing the behavior of different glass ceramic samples have been proposed. Various resistances *R*'s, capacitances *C*'s and relaxation times,  $\tau$ 's have been determined. Distribution of  $\tau$ 's for different circuit elements of the equivalent circuit model showing the electrical characteristics of glass ceramic samples were discussed.

## Results and discussion

### XRD analysis

The composition  $x = 0.2$ , has a tetragonal crystal structure at room temperature. The heat treatment schedule and nomenclature of glass ceramic samples are listed in Table 1. Figure 1 depicts the XRD patterns of the glass ceramic samples PTL7B663S, 9PL7B680S, and 8PL7B775S with  $x = 1.0, 0.9$ , and  $0.8$ , respectively. All three glass ceramic samples were obtained by crystallization of the parent glasses PTL7B, 9PL7B, and 8PL7B by heat treatment for 6 h. Perovskite  $\text{PbTiO}_3$  crystallizes as a major phase with secondary phase of  $\text{PbTi}_3\text{O}_7$  for the glass ceramic sample PTL7B, while for both remaining glass ceramic samples perovskite PST crystallizes as a major phase with secondary phase of  $\text{PbTi}_3\text{O}_7$ . XRD patterns of the glass ceramic samples 7PL7B790S, 6PL7B796S, and 5PL7B781S crystallize at three different temperatures for 6 h are shown in Fig. 2a–c. Perovskite PST crystallizes as a major phase for all the three glass ceramic samples. XRD pattern of glass ceramic sample 7PL7B790S with  $x = 0.70$  shows intense peaks of secondary phase of  $\text{PbTi}_3\text{O}_7$ . XRD pattern of the glass ceramic sample 6PL7B796S depicts a low intensity peak of secondary phase of  $\text{PbTi}_3\text{O}_7$ . Figure 2c shows the XRD pattern of glass ceramic sample 5PL7B781S crystallized for 6 h. It is observed from XRD pattern of this glass ceramic sample that  $\text{PbTi}_3\text{O}_7$  and  $\text{TiO}_2$  (rutile) crystallize as secondary phases. Crystal structure, lattice parameters and axial ratio of major crystalline phase of different glass ceramic samples are listed in Table 2.

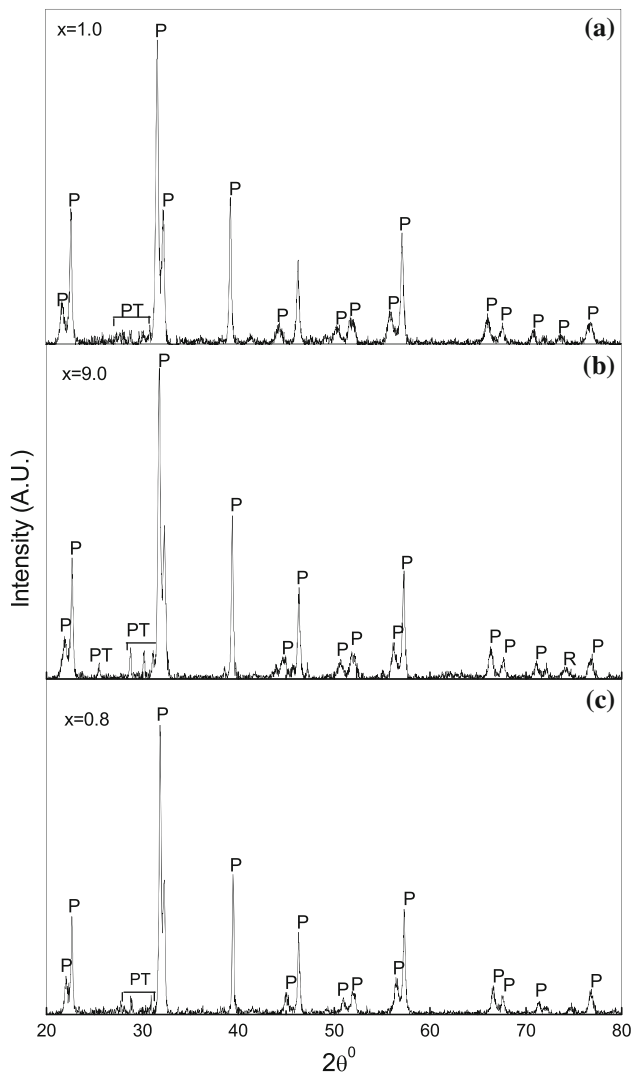


**Fig. 1** X-ray diffraction patterns of different glass ceramic samples: **a** PTL7B663S, **b** 9PL7B680S, and **c** 8PL7B775S

#### Scanning electron microscopic studies

Figure 3a–c shows the scanning electron micrographs of glass ceramic samples 9PL7B637T, 8PL7B775T, and 5PL7B781T, respectively, heat treated for 3 h. Fine crystallites of major phase of perovskite (Pb, Sr)TiO<sub>3</sub> are randomly dispersed in the glassy network and agglomeration of the crystallites is also observed in these micrographs. In Fig. 3a, b, the crystallites of secondary phase of PbTi<sub>3</sub>O<sub>7</sub> were clearly seen. These crystallites of secondary phase of PbTi<sub>3</sub>O<sub>7</sub> have the larger size in comparison to crystallites of major phase of perovskite PST. SEM of the glass ceramic sample 5PL7B781T (Fig. 3c) indicates the presence of uniform and interconnected agglomerated crystallites.

Figure 4a–d shows scanning electron micrographs of some representative glass ceramic samples. Micrometer or

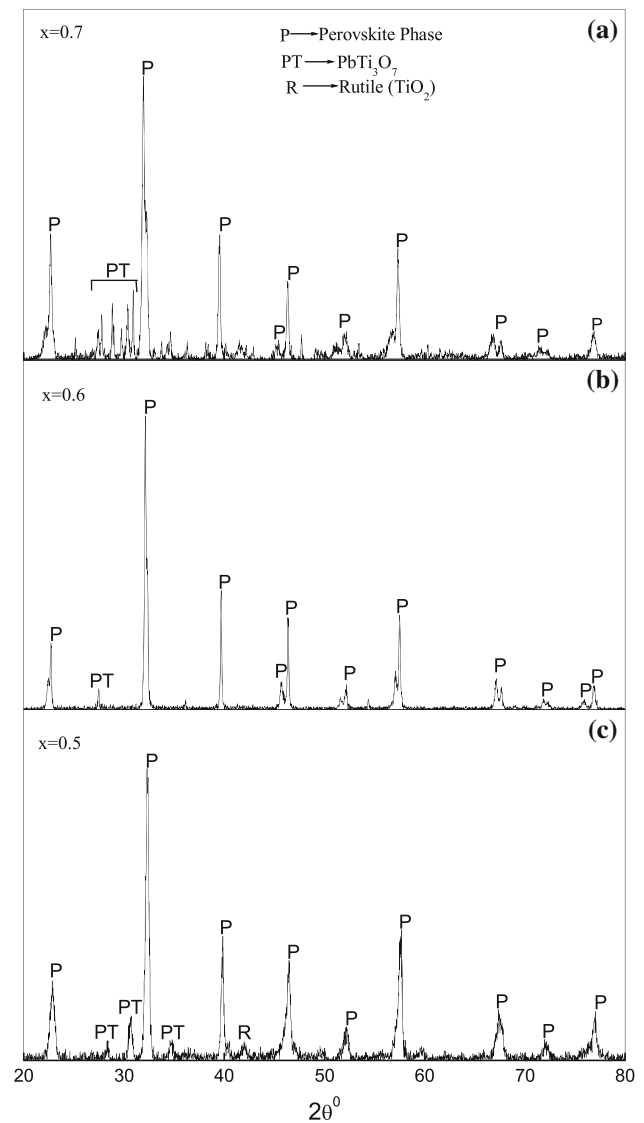


**Fig. 2** X-ray diffraction patterns of different glass ceramic samples: **a** 7PL7B790S, **b** 6PL7B797S, and **c** 5PL7B781S

sub-micrometer fine grains of perovskite SrTiO<sub>3</sub> form during crystallization. In most of the cases, these grains show agglomeration and dense microstructure regions with some glassy region in-between. This type of microstructure is normally observed for those glass ceramics, which show initial phase separation before crystallization. Two regions depict different tendency of crystallization during heat treatment. The region with higher tendency of crystallization occupies greater volume with respect to the region, which do not crystallize and remains glassy. Two types of microstructure were observed for these glass ceramic samples. One is uniformly distributed fine grained microstructure and the second is phase separated fine grained microstructure. Figure 4a shows the SEM image of glass ceramic sample PTL7B663S. The bright grains inside the

**Table 2** Crystal structure, lattice parameters and axial ratio of major crystalline phase in different glass ceramic samples in the system  $64[(\text{Pb}_x\text{Sr}_{1-x})\text{O}\cdot\text{TiO}_2]-25[2\text{SiO}_2\cdot\text{B}_2\text{O}_3]-7[\text{BaO}]-3[\text{K}_2\text{O}]-1[\text{La}_2\text{O}_3]$ 

Glass ceramics	Crystal structure	Lattice parameters		Axial ratio ( $c/a$ )	PbTiO <sub>3</sub> ceramic <sup>a</sup>		
		$c$ (Å)	$a$ (Å)		$c$ (Å)	$a$ (Å)	$c/a$
PTL7B663S	Tetragonal	$4.115 \pm 0.005$	$3.912 \pm 0.004$	1.052	4.138	3.892	1.063
9PL7B680S	Tetragonal	$4.052 \pm 0.008$	$3.913 \pm 0.008$	1.035	4.004	3.837	1.043
8PL7B775S	Tetragonal	$4.031 \pm 0.0008$	$3.912 \pm 0.0008$	1.030	3.983	3.864	1.030
7PL7B790S	Tetragonal	$4.028 \pm 0.004$	$3.908 \pm 0.004$	1.030	3.984	3.903	1.020
6PL7B797S	Tetragonal	$4.123 \pm 0.010$	$3.906 \pm 0.009$	1.055	3.947	3.882	1.016
5PL7B781S	Tetragonal	$4.112 \pm 0.006$	$3.915 \pm 0.006$	1.050	3.960	3.896	1.016

<sup>a</sup> Ref. [31]

micrographs show the major phase of the perovskite PbTiO<sub>3</sub>, while dark region may show the residual glass embodied around the fine crystallites of the major phase. These fine crystallites are interconnected and uniformly distributed in the glassy matrix. It is also observed that the secondary phase of PbTi<sub>3</sub>O<sub>7</sub> agglomerated at surfaces of the crystallites and appears brighter. These crystallites of secondary phase have the large crystallites size in comparison to that of the crystallites of major phase of perovskite PST. Figure 4b shows the SEM image of the glass ceramic sample, 8PL7B775S. Very fine and dense crystallites of perovskite PST are uniformly dispersed in glassy matrix. It is also observed that secondary phase of PbTi<sub>3</sub>O<sub>7</sub> crystallites are crystallized. The crystallites of PbTi<sub>3</sub>O<sub>7</sub> are found large in size as compared to major phase crystallites. Figure 4c shows the SEM image of the glass ceramic sample 6PL7B796S with composition  $x = 0.6$  for 6 h. Perovskite PST crystallizes as a major phase for this glass ceramic sample. SEM image of the glass ceramic sample 5PL7B881S (Fig. 4d) indicates that uniform and interconnected crystallites of the major phase of PST. However, the crystallites are fully developed within glassy matrix. The agglomeration of the crystallites was observed for the SEM image of glass ceramic sample 5PL7B881S (see Fig. 4d). This agglomeration of the crystallites is brighter and appears white in color. In order to have insight of the microstructure and confirm the phase contrast of different phases present in the sintered samples, the Backscattered SEM image of various compositions should be recorded, however, due to limited facility we could not perform these measurements.

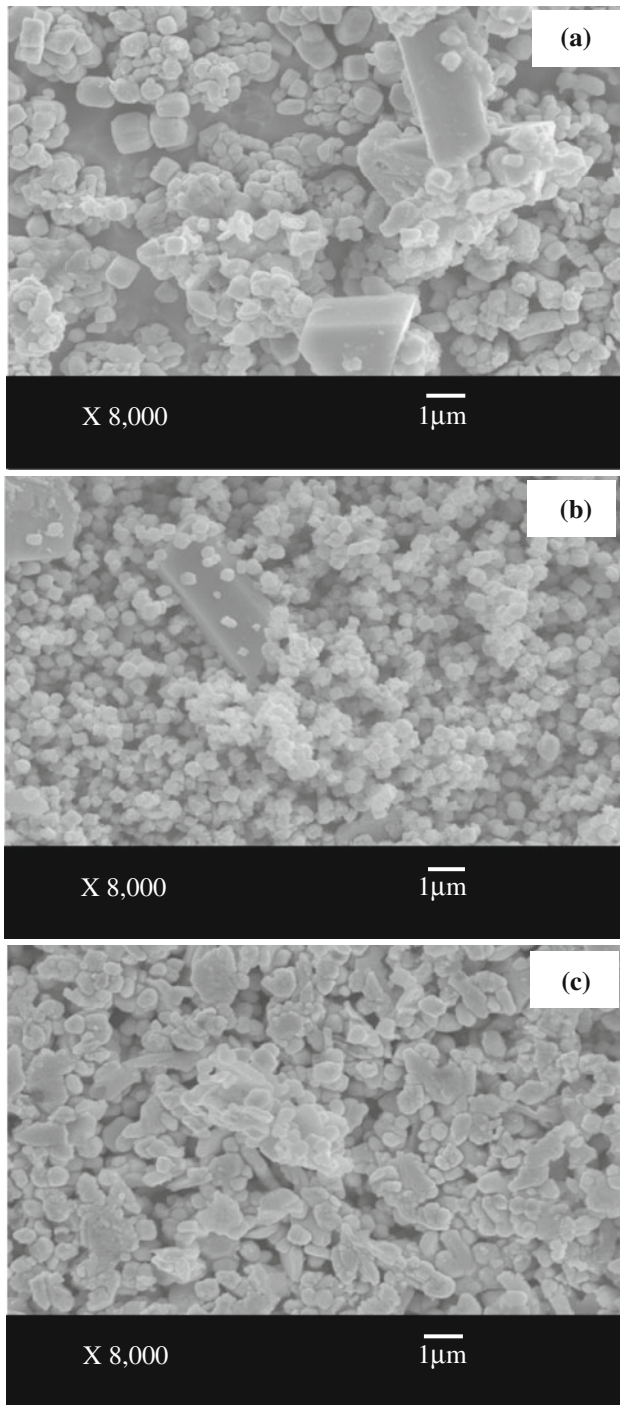
### Dielectric behavior

Figure 5 shows the variation of dielectric constant ( $\epsilon_r$ ) and dissipation factor ( $D$ ) with temperature at a few selected frequencies for the glass ceramic sample PTL7B663S. The dielectric constant,  $\epsilon_r$  remains constant up to a certain temperature thereafter it increases rapidly.  $\epsilon_r$  and  $D$  at RT

and at 1 kHz for glass ceramic sample PTL7B663S have been found to be 47 and 0.0071, respectively. A peak in  $\epsilon_r$  versus  $T$ , is observed at all frequencies. Since the  $\epsilon_r$  increases rapidly with increasing temperature around this frequency, these peaks seem to be shifted toward the higher temperature side followed by rapid increase of  $\epsilon_r$ , due to an increase in space charge polarization. The variation of  $D$  versus  $T$ , also shows a peak. After this peak, the dielectric loss again increases rapidly with increasing temperature due to the motion of the alkali ions. Figure 6 depicts the  $\epsilon_r$  versus  $T$  plots for the glass ceramic sample 8PL7B775S. Relaxation peaks were observed in both  $\epsilon_r$  and  $D$  versus  $T$  plot. A frequency-dependent broad dielectric peak is observed, which indicates that some relaxation polarization mechanism is operative in these glass ceramics. The inverse of frequency represents the relaxation time,  $\tau$  of the polarization process at the peak temperature. Plots of  $\log \tau$  versus  $1/T$  for the glass ceramic sample 8PL7B775S is shown in Fig. 7. The plot is found to be linear obeying Arrhenius relationship.

$$\tau = \tau_0 \exp\left(\frac{E_A}{kT}\right)$$

where  $E_A$  is the activation energy for the relaxation process. Value of  $E_A$  for this glass ceramic sample is determined as 0.482 eV. In these glass ceramics, the peak in their  $\epsilon_r$  versus  $T$  plots occurs close to  $T_c$ , for the corresponding Pb<sub>0.8</sub>Sr<sub>0.2</sub>TiO<sub>3</sub> solid solution ceramic composition (Table 3) [31]. The presence of similar peak in  $\epsilon_r$  versus  $T$  plot for these glass ceramic samples is attributed to ferroelectric to paraelectric transformation. It is observed that the  $T_c$ , peak of the crystallites is embedded in the glassy matrix.  $\epsilon_r$  versus  $T$  and  $D$  versus  $T$  plots of the glass ceramic sample 6PL7B796S is shown in Fig. 8a, b. Very high value of  $\epsilon_r$  was observed in this glass ceramic sample. Large value of  $\epsilon_r$  is attributed to space charge polarization due to the conductivity difference between the crystallized phase of perovskite PST and residual glassy matrix. Figure 9 represents the dielectric and loss behavior



**Fig. 3** Scanning electron micrographs of glass ceramic samples: **a** 9PL7B637T, **b** 8PL7B775T, and **c** 5PL7B781T

of the glass ceramic sample 5PL7B781S. At low frequencies (0.1–1 kHz),  $\epsilon_r$  and  $D$  are steeply rising up to a certain temperature and then a broad peak is observed at both frequencies. The high values of  $\epsilon_r$  in these glasses ceramic samples are due to the addition of lanthanum oxide ( $\text{La}_2\text{O}_3$ ) and mainly depending on the semiconducting nature of the glass ceramics. The value of  $T_c$ , and  $\epsilon_r$  at

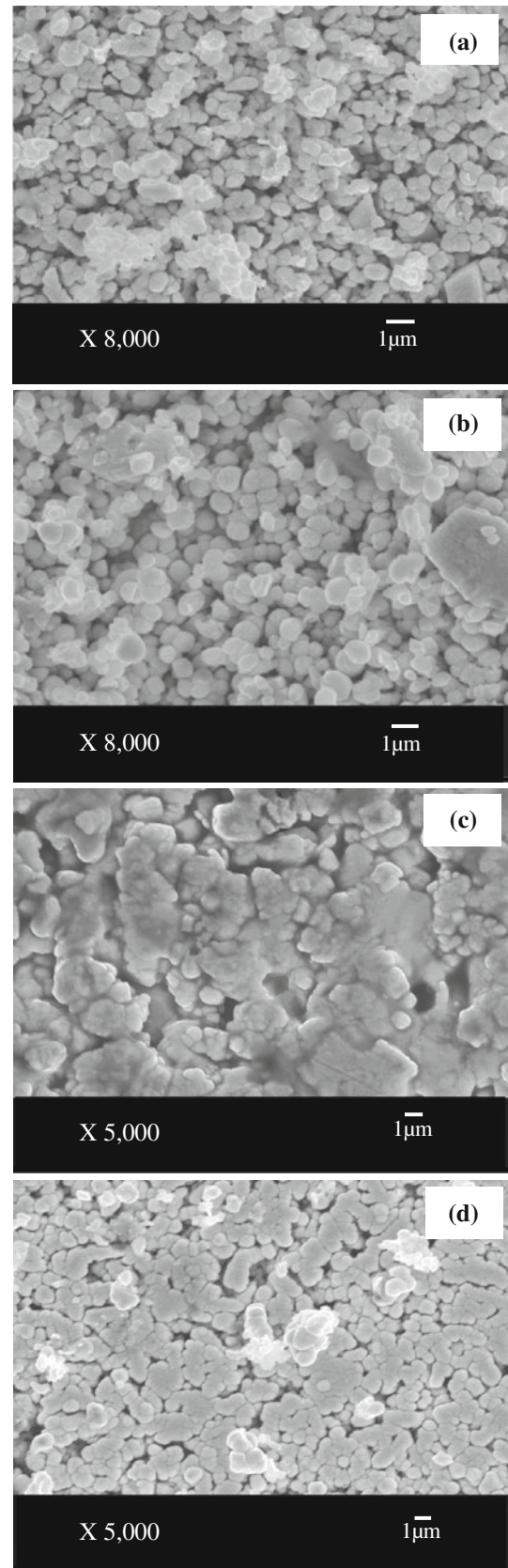


**Fig. 4** Scanning electron micrographs of glass ceramic samples: **a** PTL7B663S, **b** 8PL7B775S, **c** 6PL7B796S, and **d** 5PL7B781S

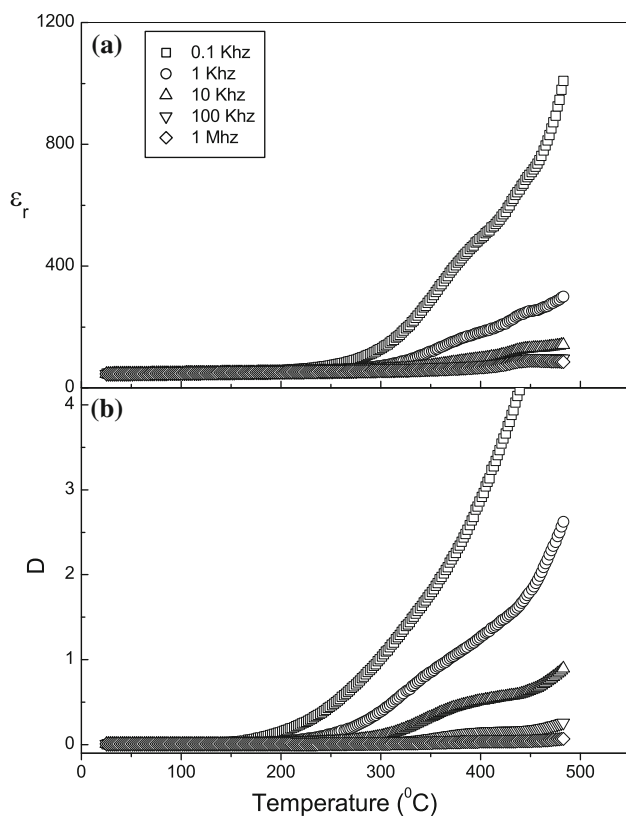
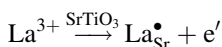
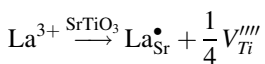


**Fig. 5** Variation of **a** dielectric constant,  $\epsilon_r$  and **b** dissipation factor,  $D$ , with temperature at different frequencies for the glass ceramic sample PTL7B663S

1 kHz at room temperature are given in Table 3 for various glass ceramic samples. Small concentration of donor dopants such as  $\text{La}^{3+}$  in perovskite ceramics are known to induce an n-type semiconductivity by electronic compensation [14].



At higher concentration, titanium vacancies form for compensating  $\text{La}^{3+}$  doping



The simultaneous presence of ferroelectric to paraelectric transition and relaxation polarization increases the broadness of  $\epsilon_r$  versus  $T$  peaks with relatively large peak height. Dielectric characteristics of these glass ceramic samples are very much similar to ferroelectric relaxor materials.

#### Impedance and modulus spectroscopy

A representative glass ceramic sample, 8PL7B775S has been selected for immittance spectroscopic study because this glass ceramic sample shows dielectric behavior with

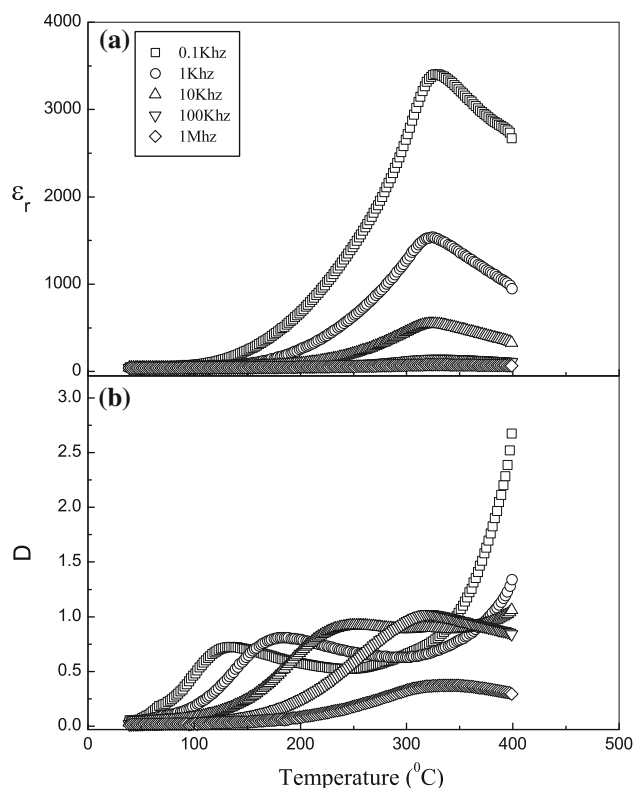


**Fig. 6** Variation of **a** dielectric constant,  $\epsilon_r$  and **b** dissipation factor,  $D$ , with temperature at different frequencies for the glass ceramic sample 8PL7B775S

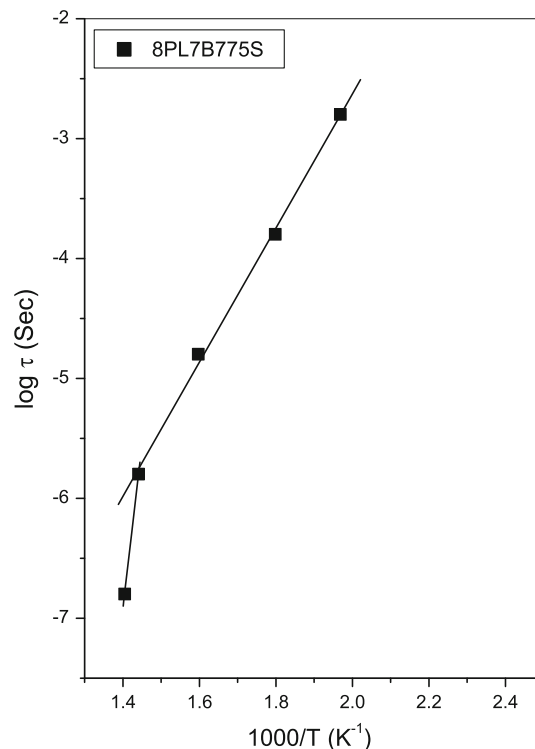


**Fig. 7** Variation of relaxation time,  $\tau$  with inverse of temperature for glass ceramic samples 8PL7B775S

**Table 3** Grain size and dielectric characteristics of the different glass ceramic samples

Glass ceramic codes	Grain size ( $\mu\text{m}$ )	$T_c$ at 1 kHz ( $^{\circ}\text{C}$ )	$\epsilon_r$ at 1 kHz at RT	$\epsilon_r$ at $T_c$	$T_c$ of $\text{Pb}_x\text{Sr}_{1-x}\text{TiO}_3$ ceramics <sup>a</sup>
PTL7B663S	1.00	–	47	–	495
9PL7B680S	0.33	393	44	675	389
8PL7B775S	0.20	323	45	1,536	323
7PL7B790S	1.00	283	58	843	283
6PL7B797S	1.40	193	3,725	8,354	211
5PL7B781S	0.56	–	52	–	120

<sup>a</sup> Ref. [31]

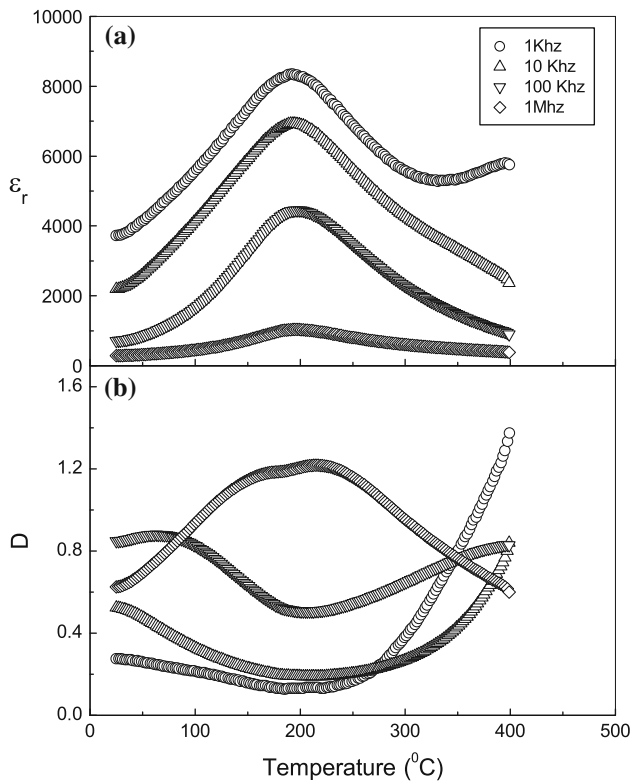


**Fig. 8** Variation of **a** dielectric constant,  $\epsilon_r$  and **b** dissipation factor,  $D$ , with temperature at different frequencies for the glass ceramic sample 6PL7B796S

well-resolved relaxation peaks in their  $D$  versus  $T$  plots. Figure 10 shows immittance spectroscopy plots ( $Z''$  vs.  $\log f$  and  $M''$  vs.  $\log f$ ) for the glass ceramic sample 8PL7B775S.  $Z''$  increases very rapidly with decreasing frequency due to the motion of the alkali ions. Generally  $Z''$  plots do not show a peak; only at high temperature, a peak is observed because it appears that the peak at lower temperatures is beyond the lowest available frequency range.  $M''$  plots for this glass ceramic sample show a broad peak which shifts to high frequency side with increasing temperature. In  $Z''$  versus  $\log f$  and  $M''$  versus  $\log f$  spectroscopic plots a peak is observed at a frequency where a polarization process shows a relaxation. The height of  $Z''$

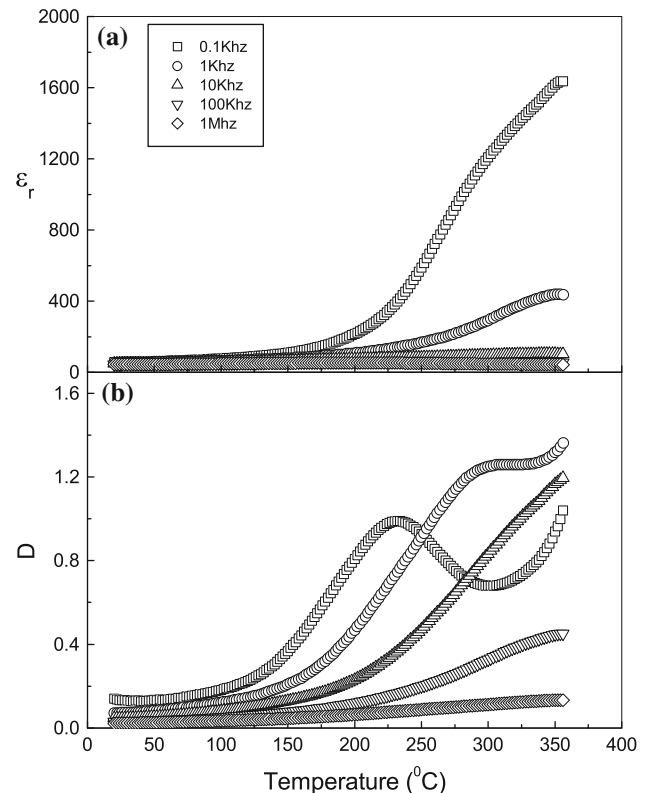


**Fig. 9** Variation of **a** dielectric constant,  $\epsilon_r$  and **b** dissipation factor,  $D$ , with temperature at different frequencies for the glass ceramic sample 5PL7B781S

peak is proportional to resistance  $R$  of the equivalent circuit corresponding to the polarization process. The height of the  $M''$  peak is proportional to the modulus, i.e., inverse of  $\epsilon_r$ . Hence,  $Z''$  plots show the most resistive contribution of the equivalent circuit model and  $M''$  plots highlight the least capacitive contribution of the equivalent circuit. In these glass ceramic samples  $\text{La}_2\text{O}_3$  has been added as an additive. La ions can diffuse into the solid solution crystallites of PST making them semiconducting.  $\text{La}_2\text{O}_3$  doping in  $\text{SrTiO}_3$  leads to the formation of electronic defects and/or vacancies of titanium cation, depending on the doping level and processing condition as present in the following equations, where all symbols are in Kröger–Vink notations.



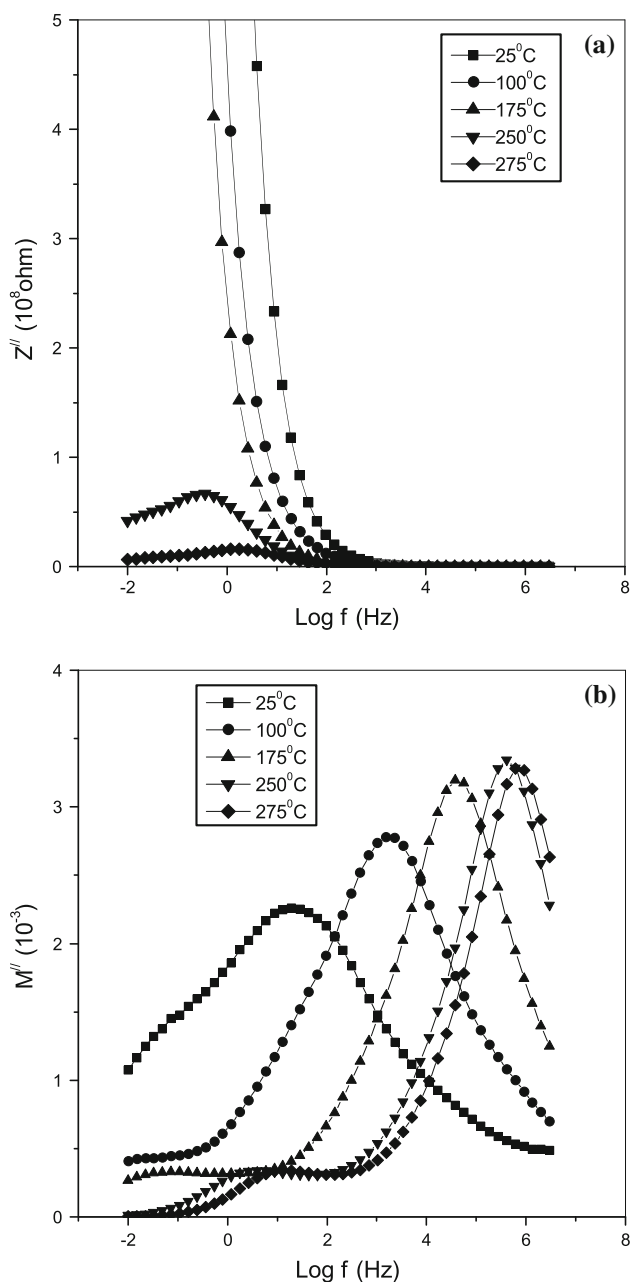
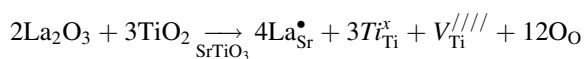
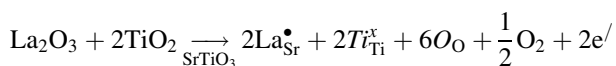


**Fig. 10** Variation of **a**  $Z''$ , **b**  $M''$  with  $\log f$  at some steady temperatures for the glass ceramic sample 8PL7B775S



The interface between semiconducting crystalline phase and insulating glassy matrix is highly resistive and space charge polarization develops at this interface. The variation of  $Z''$  and  $M''$  with  $\log$  frequency at 25 and 250 °C for glass ceramic sample 8PL7B775S, plotted in a combined manner is shown in Fig. 11. These plots indicate that two distinct

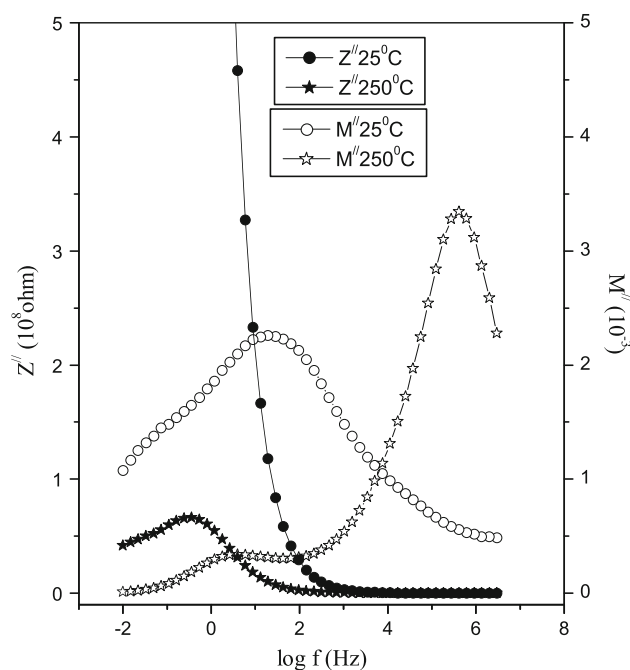


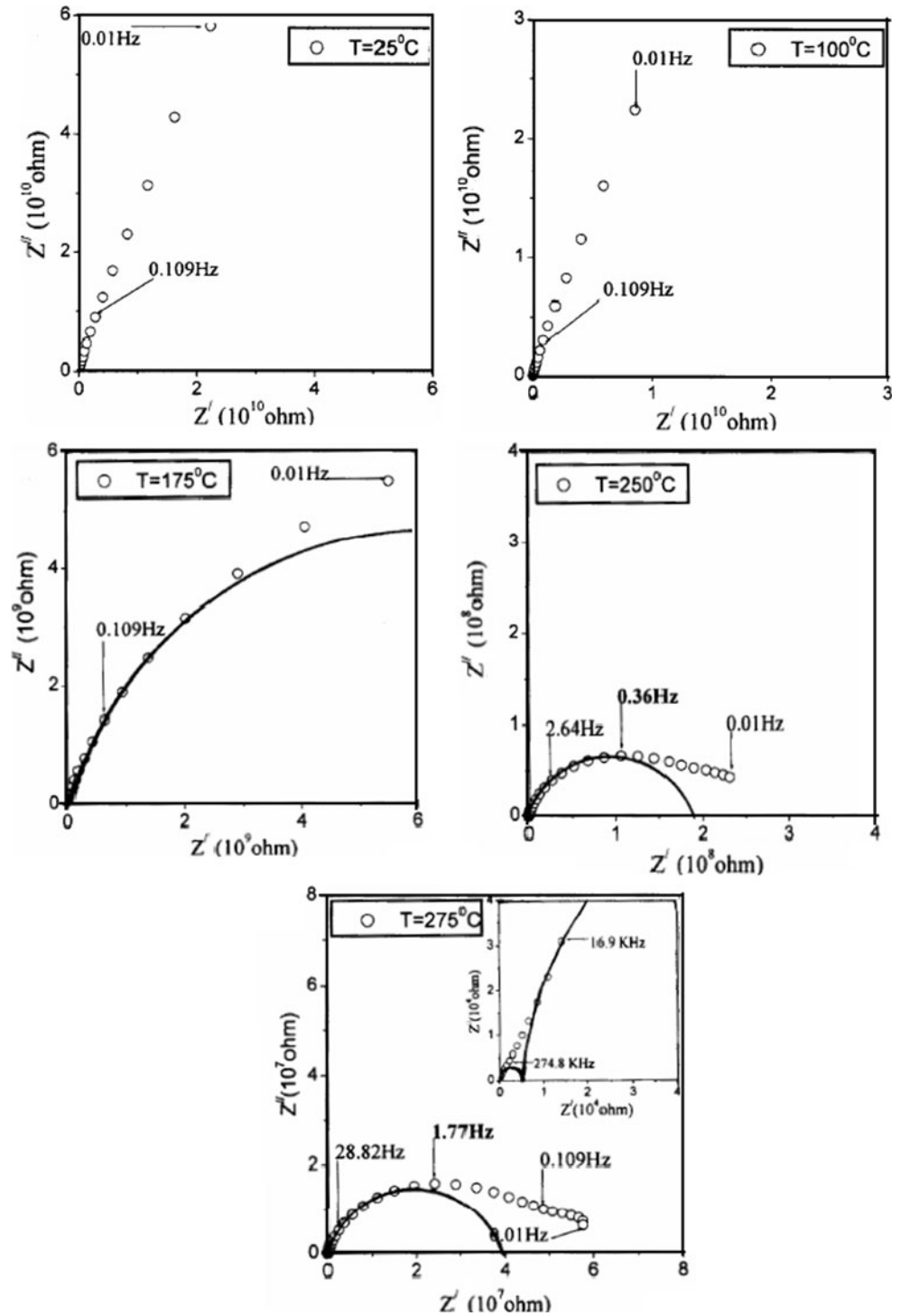
**Fig. 11** Variation of **a**  $Z''$  and **b**  $M''$  with  $\log f$  at 25 and 250 °C for the glass ceramic sample 8PL7B775S

polarization processes are present. The polarization processes relaxing at low frequencies is resistive in nature with high value of associated capacitance,  $C$ , whereas the polarization process relaxing at high frequencies contributes to low value of resistance  $R$  and  $C$ . The  $R$  for both the contributions decreases exponentially with  $T$ . Two peaks are observed in  $M''$  versus  $\log f$  plots. The peak height of low frequency peak decreases with increasing  $T$ , whereas height of high frequency peak increases with increasing,  $T$ .  $M''$  is inversely proportional to dielectric constant, polarization, or capacitance, and thus interface polarization corresponding to low frequency with increasing  $T$ . This observation is in conformity with the dielectric behavior of this glass ceramic. Hence, it can be concluded that in these glass ceramic samples, there are three contributions to the polarization processes. Because of these three types of polarization processes contributing to total dielectric behavior,  $D$  versus  $T$  plots for these glass ceramic samples either do not show any peak or show a very broad peak.

#### Complex plane impedance and modulus analysis

Complex impedance plots ( $Z''$  vs.  $Z'$ ) for glass ceramic sample 8PL7B775S at different temperatures are shown in Fig. 12. At lower  $T$ , there is a steeply rising arc indicating that the resistive contribution of one of the polarization processes (interface) is very high, masking the resistive contributions to other polarization processes. By comprising

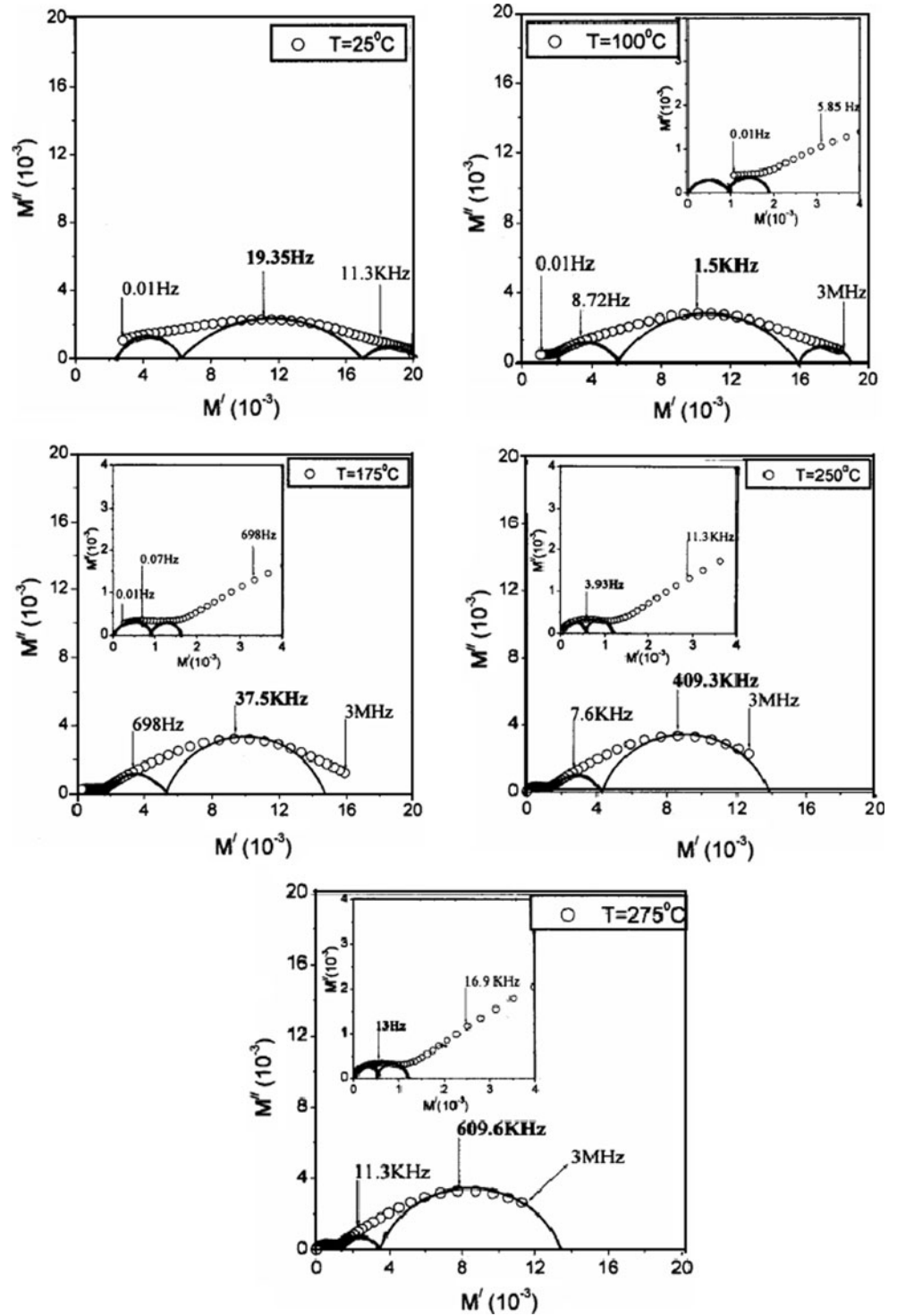
**Fig. 12** Complex impedance,  $Z''$  vs.  $Z'$ , plots at a few selected temperatures for the glass ceramic sample 8PL7B775S



these plots with simulated patterns [32], it can be ascertain that the equivalent circuit must contain a high value of blocking electrodes capacitor. It is well known that the information at higher frequency side is relatively suppressed in impedance plots, whereas it is highlighted in modulus plots [33]. Therefore, the impedance data for this glass

ceramic sample would be analyzed in electric modulus formalism. Complex modulus plots for glass ceramic sample 8PL7B775S is shown in Fig. 13. There is one highly depressed arc at lower temperature. With increasing temperature, another arc starts appearing in the low frequency range near the origin. The intercept of these arcs ( $Z''$  vs.

**Fig. 13** Complex modulus,  $M''$  versus  $M'$ , plots at a few selected temperatures for the glass ceramic sample 8PL7B775S



$Z'$  and  $M''$  vs.  $M'$  represents the resistive and inverse of the capacitive contributions of different polarization processes, respectively. The resistive and capacitive contributions of polarization processes relaxing in the low frequency range are higher in comparison to those of the polarization processes relaxing in the high frequency range. Because the

glass ceramic sample consists of fine crystallites of tetragonal PST phase dispersed in the glassy matrix. The glassy matrix is continuous and the total resistance of the glass ceramic sample is high indicating the presence of insulating glassy matrix. Since the titanate crystallites are doped with a donor dopant  $La_2O_3$ , the interface of crystal and glass blocks

the charges because of its insulating nature. This result a low resistance crystallites. Therefore, low frequency relaxation processes represent the contributions of glassy matrix and crystal to glass interface. The high frequency relaxation processes represent the contributions of the crystal phases in the glass ceramic. If we take a closer look at the complex modulus plots at different temperatures and consider the curvature of the arc in different regions, the low frequency arcs in complex impedance and modulus plots can be fitted with two circular arcs whereas the higher frequency arc can be fitted with three circular arcs. The manually fitted circular arcs are also drawn in different complex impedance and modulus plots at different temperatures wherever possible.

*R*'s and *C*'s contributions of different processes operative in these glass ceramic samples have been determined from the intercepts of the fitted arcs on *Z'* and *M'* axes, respectively. The relaxation frequency (inverse of relaxation time = *RC*) were obtained from the point of maximum of circular arc of *M''* versus *M'* plots. It has been done only in cases, where *R*'s contributions could not be determined from the complex plane impedance plots. Values of different *R* and *C* contributions are listed in Table 4.

The equivalent circuit for the Pb, rich glass ceramic sample 8PL7B775S can be modeled by mainly two parallel *RC* circuits connected in series representing the contributions of polarization processes from crystallites and the glass to crystal interface. Each parallel *RC* circuit can further be subdivided into two or three *RC* circuits. The separation of the *RC* contribution depends on composition, heat treatment, and the temperature of measurements.

The polarization contributions relaxing at high frequency, divided into three parts and representing the contributions of the crystalline phases in the glass ceramics may be from major crystalline and minor crystalline phases. It has been reported that La doping in ferroelectric ceramics changes the *T<sub>c</sub>*. *T<sub>c</sub>* decreases with increasing La doping [34]. In these glass ceramics, La<sub>2</sub>O<sub>3</sub> addition enhances the crystallization of perovskite phase, and hence serves as a nucleating agent. La ions might not be distributed homogeneously. Because of non-uniform distribution of La ions, different regions of the crystallites in the glass ceramic sample may have different *T<sub>c</sub>* and also different conductivity. This may lead to different polarization processes in different regions of crystallites, which may give rise to relaxor-like behavior with high value of *ε<sub>r</sub>* in these glass ceramic samples. The glass ceramic sample also contains alkali K<sub>2</sub>O and alkaline earth oxide, BaO. It has been reported that these modifier elements are necessary for the crystallization of the perovskite phase in major amount in the glass ceramics. However, these ions are not part of the glass network and contribute to electrical conduction particularly at high temperature. This also gives

**Table 4** Values of different *R* and *C* contributions for the glass ceramic sample 8PL7B775S

Temp (°C)	<i>C</i> <sub>1</sub> (pF)	<i>R</i> <sub>1</sub> (Ω)	<i>τ</i> <sub>1</sub> (s)	<i>C</i> <sub>2</sub> (pF)	<i>R</i> <sub>2</sub> (Ω)	<i>τ</i> <sub>2</sub> (s)	<i>C</i> <sub>3</sub> (pF)	<i>R</i> <sub>3</sub> (Ω)	<i>τ</i> <sub>3</sub> (s)	<i>C</i> <sub>4</sub> (pF)	<i>R</i> <sub>4</sub> (Ω)	<i>τ</i> <sub>4</sub> (s)	<i>C</i> <sub>5</sub> (pF)	<i>R</i> <sub>5</sub> (Ω)	<i>τ</i> <sub>5</sub> (s)
25	233	$18.2 \times 10^3$	$4.24 \times 10^{-6}$	71.5	$5.18 \times 10^7$	$3.70 \times 10^{-3}$	194	$7.5 \times 10^9$	1.46	332	—	—	—	—	—
100	273	$1.01 \times 10^3$	$2.61 \times 10^{-7}$	77.5	$9.35 \times 10^5$	$6.90 \times 10^{-5}$	221	$5.80 \times 10^8$	$1.22 \times 10^2$	830	$3.89 \times 10^9$	3.23	893	—	—
175	—	—	—	83	$3.43 \times 10^4$	$2.85 \times 10^{-6}$	211	$7.25 \times 10^5$	$1.53 \times 10^{-4}$	$1.06 \times 10^3$	$1 \times 10^8$	$8.98 \times 10^{-2}$	893	$1.26 \times 10^9$	4.82
250	—	—	—	81.5	$2.19 \times 10^3$	$3.89 \times 10^{-7}$	273	$5.14 \times 10^4$	$1.40 \times 10^{-5}$	$1.29 \times 10^3$	$9.49 \times 10^6$	$1.22 \times 10^{-2}$	$1.29 \times 10^3$	$1.04 \times 10^8$	13.4
275	—	—	—	80.1	—	$1.75 \times 10^{-7}$	387	$2.43 \times 10^4$	$9.42 \times 10^{-6}$	$1.16 \times 10^3$	$2.14 \times 10^6$	$2.42 \times 10^{-3}$	$1.66 \times 10^3$	$1.64 \times 10^7$	$2.72 \times 10^{-2}$

rise to increase in the value of  $D$  with increasing temperatures in the high temperature range.

## Conclusion

Bulk transparent glasses were prepared in the glass ceramic system  $64[(\text{Pb}_x\text{Sr}_{1-x})\text{O}\cdot\text{TiO}_2]-25[2\text{SiO}_2\cdot\text{B}_2\text{O}_3]-7[\text{BaO}]-3[\text{K}_2\text{O}]-1[\text{La}_2\text{O}_3]$  with addition of 1 mol%  $\text{La}_2\text{O}_3$  ( $0.5 \leq x \leq 1$ ). Perovskite PST is found to crystallize as major phase for all glass ceramic samples. Pyrochlore phase of  $\text{PbTi}_3\text{O}_7$  is found to crystallize in Pb rich compositions. It has also been observed that presence of BaO favors the formation of good transparent glasses, whereas presence of  $\text{K}_2\text{O}$  favors crystallization of perovskite titanate phase. The fine crystallites are found to be uniformly distributed in the glassy matrix. Enhanced crystallization is observed for 6.0 h heat treatment schedule. The high value of  $\epsilon_r$  is attributed to space charge polarization. Glass ceramic sample 6PL7B796S showing high value of  $\epsilon_r$  with small temperature dependence may find application in ceramic capacitor industry. It is also observed that the value of  $\epsilon_r$  is less for the glass ceramic sample PTL7B663S. The contributions of the polarization process relaxing in the low frequency region are due to polarizations at the crystal to glass interface and the glassy region. The model equivalent RC circuit element representing the polarization process relaxing in the low frequency region can be subdivided into two RC elements.

**Acknowledgements** The authors would like to thank the Defence Research Development Organisation, India for financial support and to Prof. D. Pandey of School of Materials Science and Technology, IT-BHU, for providing XRD facility.

## References

1. McMillan PW (1979) Glass ceramics. Academic Press, New York
2. Kang DH, Kim JH, Park JH, Yoon KH (2001) Mater Res Bull 36:265–267
3. MacDonald JR (1987) Impedance spectroscopy. Wiley, New York
4. Gerhardt R, Nowick AS (1986) J Am Ceram Soc 69:641
5. Thakur OP, Kumar D, Parkash O, Pandey L (1995) Bull Mater Sci 18:577
6. Thakur OP, Kumar D, Parkash O, Pandey L (1995) Mater Lett 23:253
7. Thakur OP, Kumar D, Parkash O, Pandey L (1997) Indian J Phys 71A:161
8. Thakur OP, Kumar D, Parkash O, Pandey L (1997) Bull Mater Sci 20:67
9. Sahu AK, Kumar D, Parkash O (2003) Br Ceram Trans 102:139
10. Sahu AK, Kumar D, Parkash O (2006) J Mater Sci 41:2075. doi: [10.1007/s10853-006-3642-3](https://doi.org/10.1007/s10853-006-3642-3)
11. Sahu AK, Kumar D, Parkash O, Thakur OP, Prakash C (2003) Br Ceram Trans 102:148
12. Sahu AK, Kumar D, Parkash O, Thakur OP, Prakash C (2006) J Mater Sci 41:2087. doi: [10.1007/s10853-006-3153-2](https://doi.org/10.1007/s10853-006-3153-2)
13. Prakash Om, Thakur OP (1997) Ph. D. Thesis, Banaras Hindu University, Varanasi
14. Kumar D, Gautam CR, Parkash O (2006) Appl Phys Lett 89:112908
15. Hipple VK (1995) In: Dielectrics and waves. Artech House, London
16. Hench LL (1968) In: Proc 14th Symp. Soc. Arosp. Matter Process Engg. 22
17. Isard JO (1970) J Non-Cryst Solids 4:357–365
18. Macedo PB, Bose R, Provenzano V, Litowitz TA (1972) In: Douglas RW, Ellis B (eds) Amorphous materials, vol 13. Interscience, London, p 179
19. Bergeron CG, Russell CK (1965) J Am Ceram Soc 48:115
20. Grossman DG, Isard JO (1969) J Am Ceram Soc 52:230
21. Grossman DG, Isard JO (1969) J Mater Sci 4:1059. doi: [10.1007/BF00549844](https://doi.org/10.1007/BF00549844)
22. Lynch SM, Shelby JE (1984) J Am Ceram Soc 67:424
23. Kokubo T, Tashiro M (1973/1974) J Non-Cryst Solids 13:328
24. Mianxue WU, Peinan ZHU (1986) J Non-Cryst Solids 84:344
25. Shyu J-J, Yang Y-S (1995) J Am Ceram Soc 78:1463
26. Bahramia A, Ali Nematia Z, Alizadehb P, Bolandia M (2008) J Mater Process Technol 206:126
27. Golezardi S, Marghussian VK, Beitollahi A, Mirkazemi SM (2010) J Eur Ceram Soc 30:1453
28. Saegusa K (1996) J Am Ceram Soc 79:3282
29. Gautam CR, Devendra K, Parkash O (2011) Bull Mater Sci 34:1
30. Gautam CR, Kumar D, Singh P, Parkash O (2012) ISRN Spectrosc 2012:1
31. Subrahmanyam S, Goo E (1998) Acta Mater 46:817
32. Hodge IM, Ingram MD, West R (1976) J Electroanal Chem 74:125
33. Morrison FD, Sinclair DC, West AR (1999) J Appl Phys 86:6355
34. Thakur OP, Kumar D, Parkash O, Pandey L (2003) Mater Chem Phys 78:751